Journal of Electronic Materials (2024) 53:5952–5960
https://doi.org/10.1007/s11664-024-11193-8

28TH INTERNATIONAL CONFERENCE ON NUCLEAR TRACKS AND RADIATION MEASUREMENTS

Advanced Nanostructures Derived from Hybrid Composite of Polyaniline and rGO for High-Performance Supercapacitor Applications

Paramjit Singh[1] · Rashmi Saini[2] · Rajesh Kumar[2] · Pawan Kulriya[3]

Received: 15 February 2024 / Accepted: 15 May 2024 / Published online: 30 May 2024

Abstract

The intensive investigation of supercapacitors and other advanced energy storage technologies has been driven by the growing demand for portable electronic devices, electrical equipment, and hybrid electric vehicles in the transportation sector. To develop these systems, it is crucial to have electrodes capable of high energy storage, along with suitable electrolytes to facilitate ion transport or conduction. These energy storage devices, which incorporate nanostructured and compact electrodes, exhibit excellent electrochemical performance. The hybrid nanostructured composites made of carbon allotropes and conducting polymers have received much attention recently due to their possible use in supercapacitors. They are perfect candidates for energy storage applications because of their high electrical conductivity, mechanical strength, and stability. We synthesized reduced graphene oxide by a modified Hummer's method and composited it with aniline monomers by in situ chemical polymerization to fabricate nanostructured composites of polyaniline and graphene. The different samples were synthesized by varying their mass ratios followed by their characterization by different characterization techniques such as XRD, FTIR, Raman, FESEM, and cyclic voltammetry, etc.

Keywords Polyaniline · reduced graphene oxide · supercapacitors · energy storage devices

Introduction

Advanced innovations in 1D, 2D, and 3D nanostructured materials and the optimization of parameters have revolutionized research and development in the field of sustainable energy resources. The research on advanced energy storage technologies, including supercapacitors, has been intensified to address the electrochemical performance in terms of specific capacitance, recycle stability, and durability. Pseudocapacitors, divided into metal oxide and conducting polymer types based on electrode materials, play a crucial role in supercapacitor construction. Metal oxides, such as MnO_2, $CoFe_2O_4$, ZnO, SnO_2, NiO, etc., exhibit rapid and reversible redox reactions, offering a straightforward approach with low resistance and high specific capacitance.[1] However, the utilization of metal oxides does not remain cost-effective, hence the conducting polymers like polypyrrole (PPy), polyaniline (PAni), polythiophene, polyphenylenevinylene, and polyethylene dioxythiophene are favored for redox pseudocapacitors due to their cost-effectiveness, high electrical conductivity, and quick reversible oxidation–reduction processes. These materials contribute to the efficient design and performance of supercapacitors.[2]

In the realm of conducting polymers, three key aspects warrant attention: suboptimal performance, inadequate cyclic stability, and loss of active material.[3] Research suggests that refining the microstructure and morphology of conductive polymers holds the potential to improve their performance. The challenges associated with poor cyclic stability during prolonged charge–discharge processes,

✉ Paramjit Singh
psd1985@gmail.com

[1] Department of Physics, Gujranwala Guru Nanak Khalsa College, Civil Lines, Ludhiana, Punjab 141001, India

[2] University School of Basic and Applied Sciences, Guru Gobind Singh Indraprastha University, New Delhi 110078, India

[3] School of Physical Sciences, Jawaharlal Nehru University, New Delhi 110067, India

attributed in part to inferior mechanical stability leading to issues like swelling, shrinkage, and cracks, can be alleviated by integrating conductive polymers with diverse carbon materials, such as carbon black, carbon fibers, carbon aerogels, micro-porous carbon, carbon nanotubes, graphene, and fullerene.[4] Additionally, the issue of active material loss can be addressed by adopting innovative electrolytes with broader electrochemical windows. Among the above discussed carbon materials, graphene is used the most due to its larger surface area, high electrical conductivity, and higher specific capacitance. Also, compared to other conducting polymers, PAni exhibits substantially higher capacitance due to its reversible redox reaction. This particular conducting polymer and its carbon-based composite materials play crucial roles as capacitive materials in supercapacitor applications. Nevertheless, its standalone use is constrained by issues such as inadequate rate capability, limited lifespan, or insufficient capacitance,[5] but it can boost the electrochemical capacitance of carbon-based materials through their swift doping and de-doping kinetics in charge–discharge cycles. When combined with graphene as a stable and conductive underlying network, the composite attains both enhanced electrical conductivity and improved cycling stability.

Previous investigations have primarily focused on the incorporation of conducting polymers into carbon compounds. Cheng and collaborators (2011) pioneered the development of PAni nanofibers on a carbon fiber cloth through electro-deposition, revealing a weight-normalized specific capacitance of 673 F/g. The porous nature of the carbon fiber fabric facilitated electrolyte diffusion into the electrode material, establishing numerous channels for rapid ion transport.[6] Chen et al. demonstrated a specific capacitance of 716 F/g for their 3D porous graphene-based PAni.[7] Huang and colleagues crafted PAni layers deposited onto freestanding, flexible reduced graphene oxide/carbon nanotube (rGO/CNT) papers, reporting capabilities of 229 F/g, 202 F/g, 181 F/g, and 155 F/g at current densities of 0.2 A/g, 0.5 A/g, 1 A/g, and 2 A/g, respectively.[8]

Conversely, contemporary research endeavors are directed toward exploring the nanostructures of conducting polymers in conjunction with metal oxides and carbon compounds to augment the electrochemical performance of electrodes.[9] Rahman and colleagues synthesized PAni, graphene oxide (GO), and their nanocomposites with metal oxides (MO) and hexagonal boron nitride for application in supercapacitors. Their findings revealed a specific capacitance of 351 F/g, coupled with a high-power density of 4500 W/kg.[10] Guo et al. engineered a unique structure by utilizing polyaniline (PAni) as a linker to anchor NiS_2 with a hollow bowl-like configuration uniformly dispersed on the surface of GO, resulting in a noteworthy specific capacitance of 536.13 F g^{-1} at 1 A g^{-1}.[11] Upadhyay and collaborators incorporated ruthenium oxide nanoparticles and PAni nanofibers into the interplanar spaces of rGO, achieving a maximum areal capacitance of 1.66 Fcm^{-2} at a current density of 2 mA cm^{-2}.[12] Yazar et al. (2022) reported a specific capacitance of 1217 mF cm^{-2} (608.3 Fg^{-1}) for a Cl-GO-doped PAni electrode at 4 Ag^{-1}.[5] Additionally, Xu and co-workers developed free-standing rGO/carboxymethylcellulose (CMC)–PAni hybrid film electrodes, demonstrating a specific capacitance of 450 mF cm^{-2} (81.8 F g^{-1}) at 1 mA cm^{-2}. They highlighted that a robust interaction, facilitated by hydrogen bonding, between the two elements promotes the uniform and organized growth of PAni on the CMC substrate, thereby preventing detachment during the charging/discharging process.[13]

The aforementioned contemporary investigations and additional scholarly works elucidate that modifying fabrication methodologies, regulating doping parameters, and fine-tuning the mass ratio of conducting polymer to graphene can enhance mechanical stability, consequently mitigating shrinking and swelling. This optimization further refines the microstructure and morphology of the conducting polymer, ultimately elevating the specific capacitance and cyclic stability of the electrode. rGO-conducting polymer composites can be synthesized by employing various routes, such as chemical oxidation polymerization in which the conducting polymer's corresponding monomer can be polymerized using oxidizing agents like ammonium persulfate (APS) and mixing with GO to form a composite. Similarly, in situ polymerization [14] can be used, which involves the simultaneous reduction of GO to rGO with the polymerization of the monomer. Another method of synthesis of rGO-Conducting polymers composites is electrochemical deposition.[15] In this method, the monomer is deposited electrochemically on the rGO-coated substrate. There are many more such methods that have been used for the synthesis of rGO-conducting polymer composites for energy storage applications.

In this current investigation, we have reported the electrical characteristics through systematic manipulation and regulation of the mass ratio between PAni and rGO by in situ chemical polymerization. The synthesis involved the creation of rGO-PAni composites in the proportions of 1:40, 1:60, and 1:80, followed by a comprehensive characterization to assess their supercapacitive properties.

Experimental

The graphite powder was supplied by Sigma Aldrich, while the other chemicals (Aniline, H_2SO_4 and HCl) were provided by CDH. Thomas Baker furnished $KMnO_4$, H_2O_2, ammonium persulfate, and hydrazine monohydrate (80%). The GO and rGO were synthesized from pure graphite powder using a modified Hummer's method.[16] In this process, graphite powder was mixed with H_2SO_4, stirred for 2 h at 5°C, then

heated to 20°C by gradually adding $KMnO_4$. After additional heating for 4 h, the solution was diluted, heated, and stirred before adding 10 ml of 30% H_2O_2. The resulting brownish yellow precipitate was neutralized to pH 7 using a 1% HCl solution, dried at 60°C, and ground to obtain GO. Subsequently, the prepared GO was ultra-sonicated in distilled water, and 5 ml of hydrazine monohydrate was added at 98°C to yield black precipitates. Centrifugation, followed by washing with ethanol and distilled water, was employed to isolate the precipitates, which were then dried at 60°C overnight to obtain rGO.

The composites of rGO and PAni were synthesized using chemical polymerization in which a certain amount of rGO was dispersed in a 1% ethanol with the help of ultrasonication for 2 h. Aniline was added to the diluted H_2SO_4 (maintaining the mass ratio of 1:40 of rGO-PAni) and ultrasonicated it for 2 h, and, to stabilize the reaction further, the solution was cooled to 10°C, when a bluish-colored solution was obtained. Then, 0.95 g ammonium persulphate was dissolved in small amount of deionized water and ultimately added to the previously obtained solution and left for polymerization under a magnetic stirrer for 20 h, when emerald-colored precipitates were obtained. Finally, these precipitates were washed with 1% ethanol and dried overnight in a hot air oven, hence obtaining a 1:40 rGO-PAni composite. Using a similar procedure, we synthesized 1:60 rGO-PAni and 1:80 rGO-PAni composites, by changing the amount of rGO and PAni.

Raman spectroscopy was conducted with an IndiRam instrument (CTR-300 with a 532-nm Laser), while Fourier transform infrared spectroscopy (FTIR) was employed by Perkins Elmer instrument. High-resolution transmission spectroscopy (HRTEM; Tecnai G2 20 S-TWIN; FEI) was performed, offering a point resolution of 0.24 nm and line resolution of 0.14 nm. All the mentioned characterizations were executed at the Malaviya National Institute of Technology, Jaipur, India.

Results and Discussion

Fourier-Transform Infrared Spectroscopy (FTIR)

Figure 1 displays the FTIR spectra of the rGO-PAni composites with varying composite mass ratios. The composites labeled PNGP40, PNGP60, and PNGP80 correspond to the rGO-PAni ratios of 1:40, 1:60, and 1:80, respectively. The composite formation of PAni and rGO was confirmed through the various bands corresponding to different vibrational modes, such as: 574 cm^{-1} (C-S stretching vibrational mode), 667 cm^{-1} (stretching deformation of aromatic ring), 783 cm^{-1} (aromatic C-H bending for substitutional aromatic ring)[17], and 1241 cm^{-1} (carboxyl C-OH). Similar FTIR

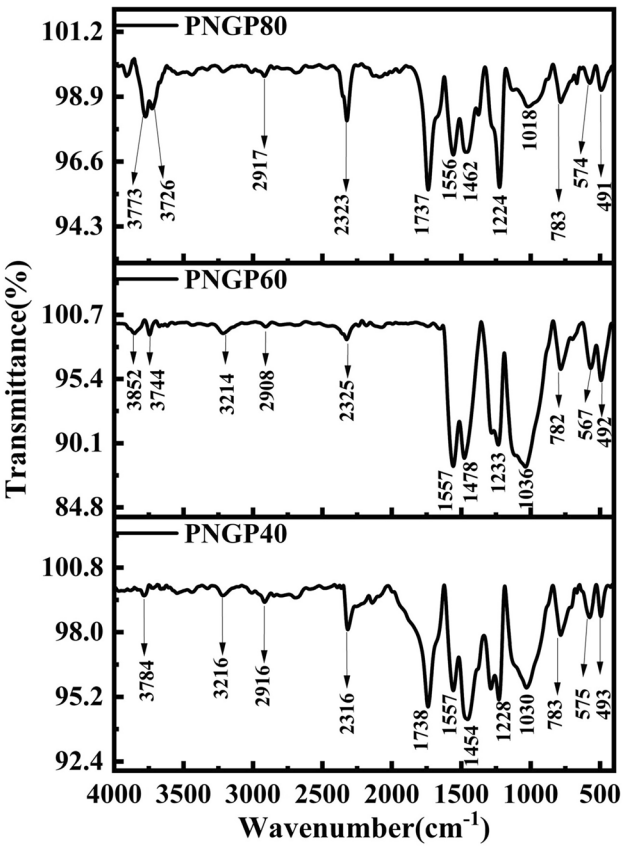

Fig. 1 FTIR spectra of rGO-PAni composites synthesized at different mass ratios.

modes were observed by Tang et al.:[17] 1280 cm^{-1} (protonation of imine nitrogen atoms of quinoid rings), 1483 cm^{-1} (C = C stretching vibration of benzoid and quinoid structures), 1560 cm^{-1} (presence of quinoid and benzenoid rings in emeraldine salt), and 1726 cm^{-1} (C = O stretching vibration of GO).[18–27] The presence of rGO was confirmed by a band at 1034 cm^{-1}[18], and another peak at 2920 cm^{-1} represents the presence of methyl groups (C-H stretching vibrations).[20] The combination of new peaks and slight variations in the position of bands were observed as one band at 3784 cm^{-1} in PNGP40, whereas two bands were observed in PNGP60 at 3852 cm^{-1} and 3744 cm^{-1} , and in PNGP80 at 3773 cm^{-1} and 3726 cm^{-1} . Similarly, some other bands also appear around higher wave numbers, due to the slight variation in the components' amount in the composites showing the change in interacting with the environment of the rGO-PAni.[28]

Raman Spectroscopy

Raman spectra of graphene-based PAni composites PNGP40, PNGP60, and PNGP80 are shown in Fig. 2, showing the characteristic vibrations of both the rGO and PAni.

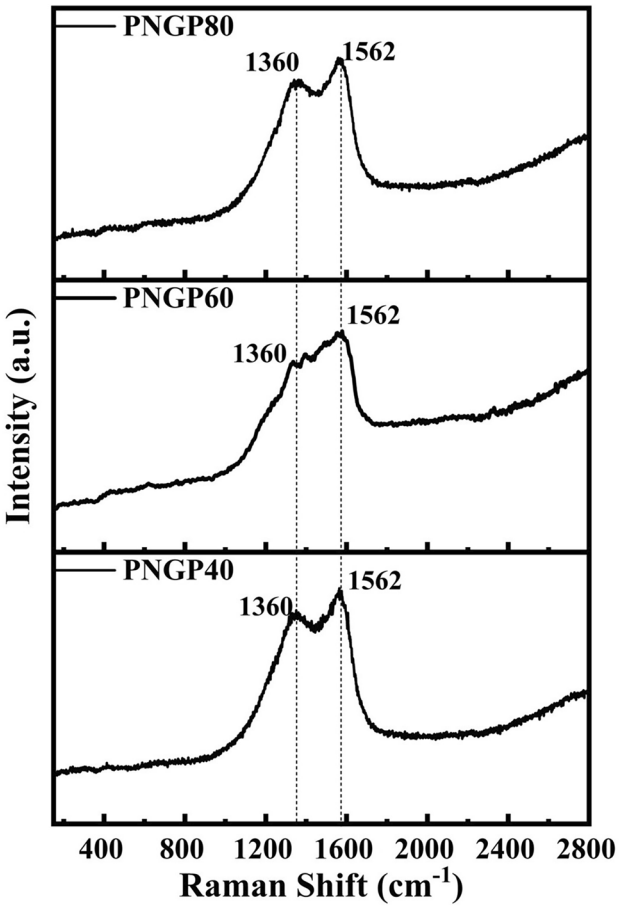

Fig. 2 Raman spectra of rGO-PAni composites synthesized at different mass ratios.

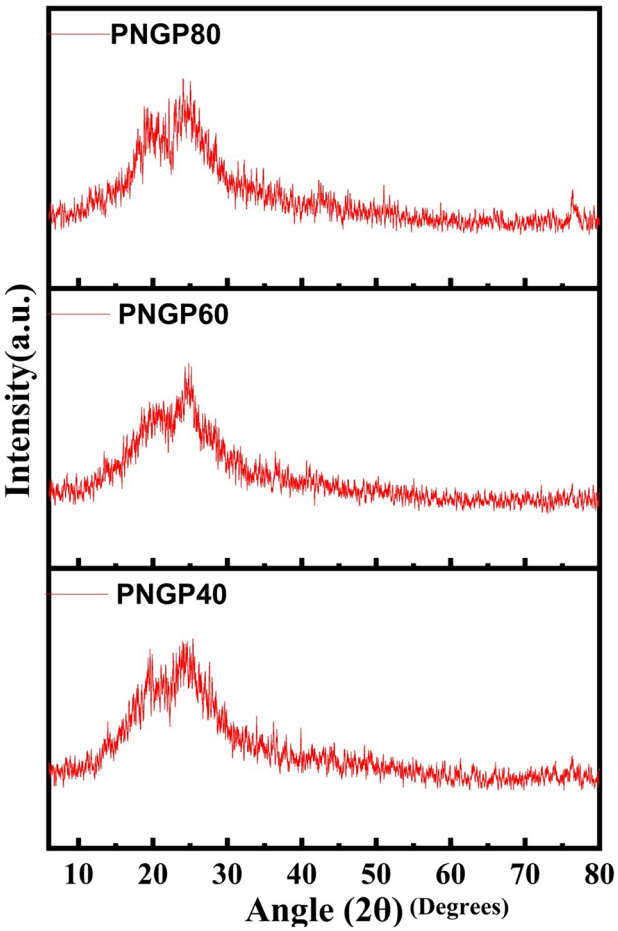

Fig. 3 XRD pattern of rGO-PAni composites synthesized at different mass ratios.

The plots show the D-band characteristic peak of the amorphous materials at 1360 cm^{-1} appearing due to the disorders created in rGO from the polymerization and attributed to the stretching vibration of the C = C bond in the quinoid ring. The D-band corresponds to the A_{1g} mode in the spectra, involving C = C bond vibrations in both the components of the composites (i.e., rGO and PAni). The peak also reveals the stretching vibration of C-N bonds. Soudagar et al. and Humpolicek et al.[29,30] reported that the G-band at 1562 cm^{-1} appeared due to the vibration of the C = C bond of the benzenoid rings present in the PAni matrix, revealing the presence of an emeraldine form.[31] According to Mitra et al.,[32] the position of the peak at 1562 cm^{-1} also corresponds to C-H vibrations in the benzenoid rings of the composite structures. The G-band corresponds to the E_{2g} mode that involves the in-plane vibrations of the C-atoms in the rGO base structure. The intensity ratio of the D-band to the G-band (I_D/I_G) observed for PNGP40 was 2.16, and 2.074 for PNGP60 and 1.253 for PNGP80. The decreased value of I_D/I_G with the variation of PAni was attributed to a more ordered or stabilized structure.[27] As the mass ratio of rGO-PAni varies and the amount of PAni is increased in the composites to1:40, 1:60, and 1:80; the reduction in the sp^2 carbon of the rGO takes place, which ultimately reduces the Raman scattering and hence the Raman intensity decreases. PAni involves the conversion of an amorphous structure to an ordered structure and hence leads to a decrease in I_D:I_G.[33,34]

X-ray Diffraction (XRD)

The XRD study was conducted to analyze the structure of the rGO-PAni composites, as shown in Fig. 3. The characteristic peaks for the composites of rGO-PAni were observed at 2θ equal to 24.67° corresponding to the (200) plane of PAni in emeraldine salt form, and the characteristic peak at 21.08° corresponding to the (002) plane of rGO.[35] The two simultaneous adjacent peaks in the XRD pattern signify the layered structure of the composites,[36] and the formation of the rGO-PAni composite that we intended to synthesize via in situ chemical polymerization reaction, while the

broadening of the peaks in the XRD pattern represent the amorphous nature of the composites.

Morphological Study

To know more about the synthesized composites, the surface morphology of the composites of rGO-PAni were studied with SEM. Figure 4 shows the SEM images for PNGP40, PNGP60, and PNGP80 at resolutions of 1 μm and 10 μm. The images of the samples exhibit the amorphous surface morphology with randomly aggregated particles over the stacking of rGO, and hence show the presence of a PAni network over the surface of rGO, revealing the in situ polymerization. Chen and his co-workers reported[37] that the introduction of rGO to the PAni enhances its electrical property. Liu et al.[38] discussed in their paper that PAni nanoparticles embedded in the rGO reinforce the charge transfer between rGO and PAni, and hence help the enhanced electrochemical performance. Dong et al.,[39] discussed the synthesis of the rGO-PAni composite to enhance the surface area by growing nanorods over the stacked rGO. Rajagopalan et al.[40] described the restacking of randomly aggregated graphene sheets with active spaces between the sheets making them capable of inducing electrolyte diffusion and hence suitable for supercapacitor application. The layered structure of the composites shown in the SEM images signify the enhanced surface area, and the few particles above the

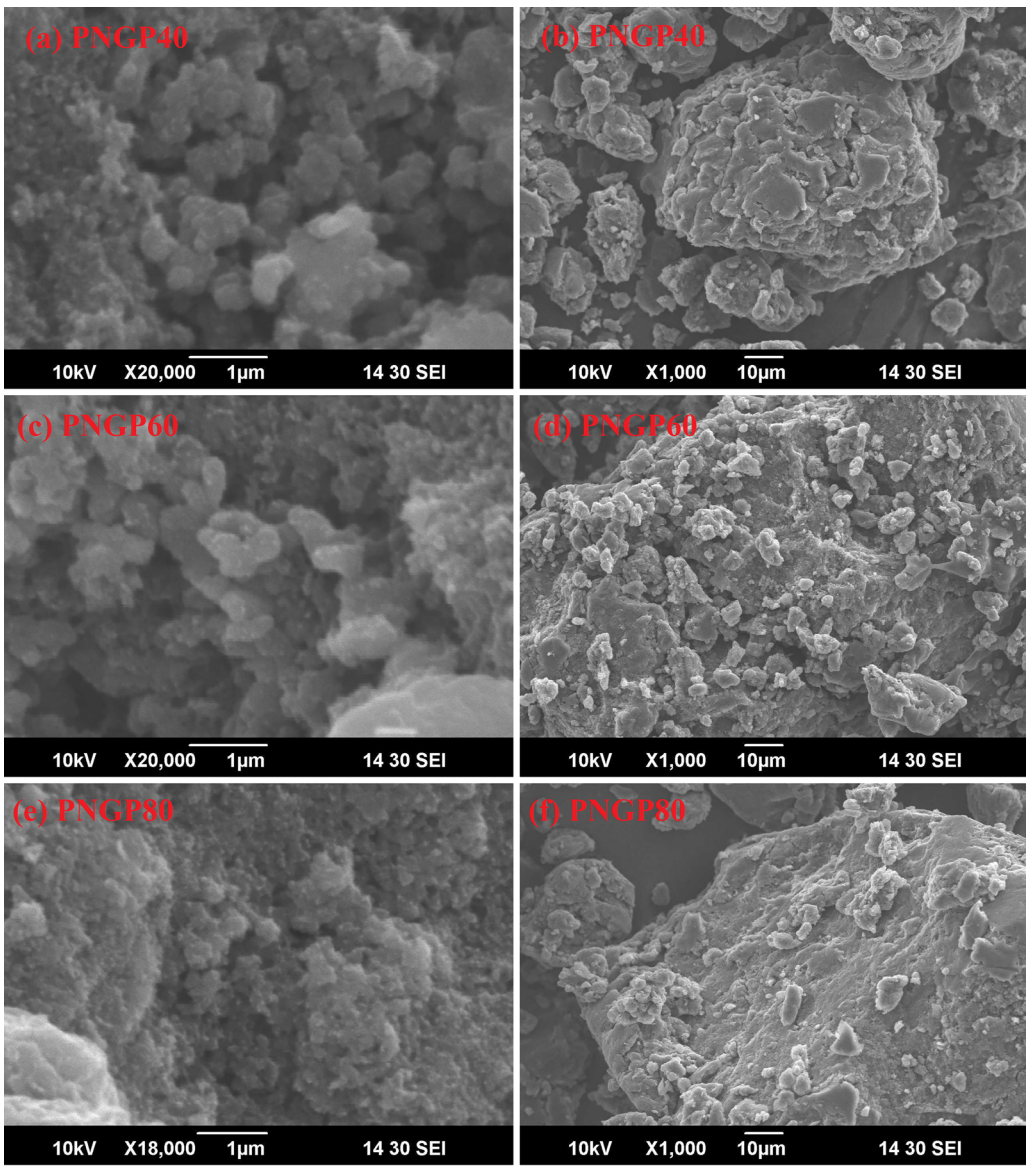

Fig. 4 SEM images of rGO-PAni composites synthesized at different mass ratios.

rGO layers represent the PAni,[41] and the different morphology depicts the varied ratio of rGO and PAni in the synthesized composites.

Electrochemical Measurements

The electrochemical performances of the graphene-based PAni composites, PNGP40, PNGP60, and PNGP80, were observed with the help of cyclic voltammetry using a three-electrode system. Figure 5 depicts the voltammograms for the synthesized pseudocapacitive materials at various scan rates ranging from 5 mV/s to 50 mV/s in the potential range of 0.2–0.8 Vm, and their symmetric cyclic plots exhibit the reversibility over a number of redox cycles and hence confirms their electrochemical stability and their efficiency for the application of supercapacitors. The specific capacitance of a material can be calculated from the voltammogram, using the relationship:[42]

$$C_{\mathrm{Sp}} = \frac{\int \mathrm{Current}}{s * \Delta V * m}$$

where s denotes the scan rate measured in mV/s, ΔV represents the potential window, and m denotes the mass of the sample material loaded on the electrode substrate. During the electrochemical measurements, the specific capacitances observed for PNGP40 are 3.18 Fg^{-1}, 3.64 Fg^{-1}, 4.32 Fg^{-1}, 5.70 Fg^{-1}, 9.49 Fg^{-1} , and 17.21 Fg^{-1} at scan rates of 5 mV/s, 10 mV/s, 20 mV/s, 30 mV/s, 40 mV/s, and 50 mV/s respectively; for PNGP60, they are 6.78 Fg^{-1}, 7.57 Fg^{-1}, 8.68 Fg^{-1}, 10.76 Fg^{-1}, 16.23 Fg^{-1} , and 27.01 Fg^{-1} at scan rates of 5 mV/s, 10 mV/s, 20 mV/s, 30 mV/s, 40 mV/s, and 50 mV/s, respectively; and for PNGP80, they are 7.77 Fg^{-1}, 7.88 Fg^{-1}, 9.03 Fg^{-1}, 10.68 Fg^{-1}, 14.80 Fg^{-1} , and 20.40 Fg^{-1} at scan rates of 5 mV/s, 10 mV/s, 20 mV/s, 30 mV/s, 40 mV/s, and 50 mV/s, respectively. Thus, the average specific capacitance for the above-mentioned scan rates is 7.26 Fg^{-1} for PNGP40, 12.84 Fg^{-1} for PNGP60, and 11.76 Fg^{-1} for PNGP80. Figure 5d shows the trends in the

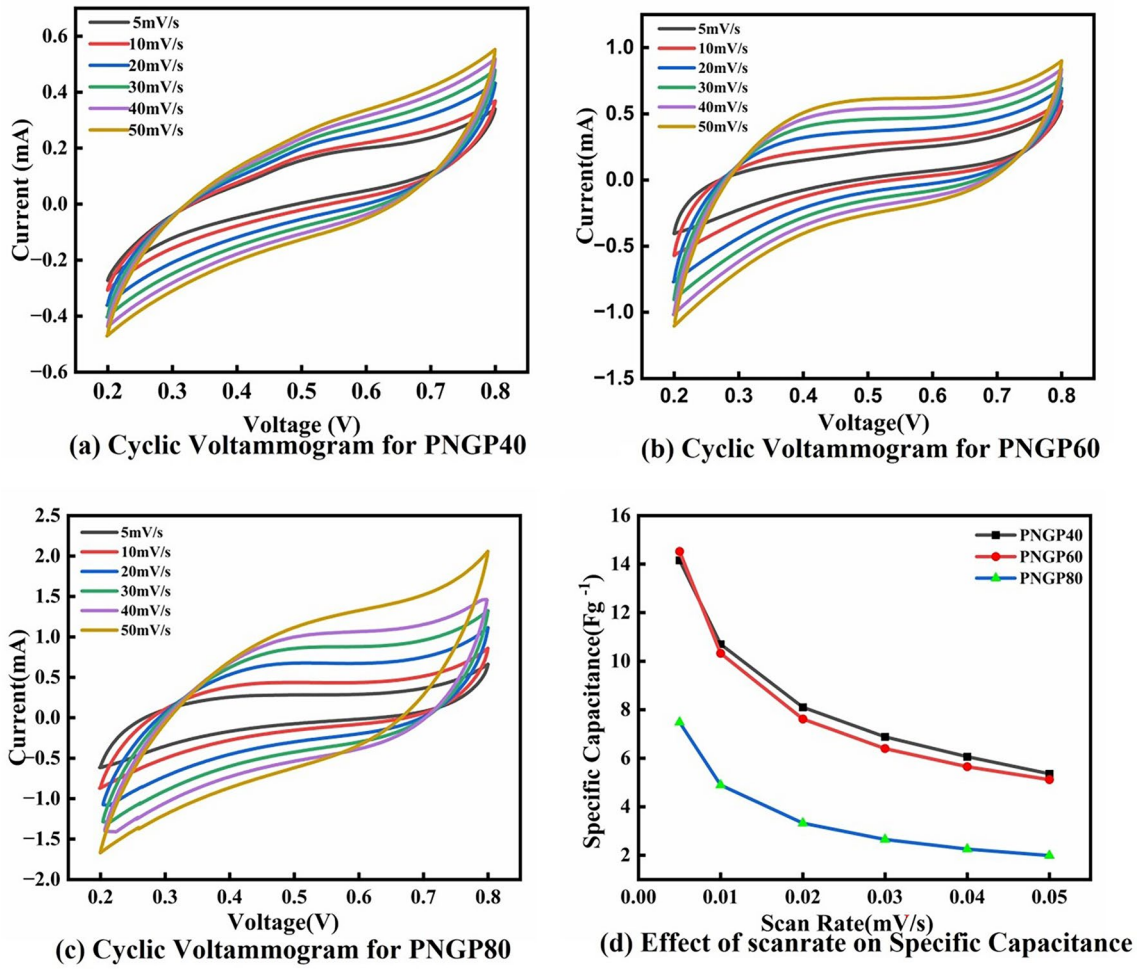

Fig. 5 Cyclic voltammetry of rGO-PAni composites synthesized at different mass ratios.

variation of specific capacitance with scan rate, revealing the decrease in specific capacitance of the sample materials with the increase in scan rate. A research group has also described the synergistic effect between rGO and PAni, due to the potential window for the redox reaction.[43] As described above in the Raman spectroscopy section, the increase of PAni content in the composites led to an ordered structure and provided better electrical conductivity, which is desirable for enhancing the capacitive performance of the supercapacitor. Among the three composites, PNGP60 exhibited the maximum gravimetric capacitance. The non-linear variation in specific capacitance of the composites is expected, due to the deviation of composition of the synthesized composites from the optimal composition. As $E = \frac{1}{2}CV^2$, therefore, with the increase of specific capacitance, the energy density also increases. However, an increase in energy density often leads to some loss of power density.[36]

Conclusions

The synthesis of rGO-based PAni nanocomposites with varying rGO to PAni mass ratios of 1:40, 1:60, and 1:80 have been carried out by in situ polymerization. The synthesized composites underwent various characterizations for the confirmation of their successful synthesis. The FTIR studies showed prominent peaks at around 574 cm^{-1}, 667 cm^{-1}, 783 cm^{-1}, 1241 cm^{-1}, 1483 cm^{-1}, 1560 cm^{-1} , etc. corresponding to various vibrational modes of chemical bonds, and hence confirmed the synthesis of the rGO-PAni composites. From the XRD patterns, peaks were observed at 21.08° and 24.67°, and the formation of semi-crystalline planes for rGO and PANi in the rGO-PAni composites at (002) and (200), respectively. Raman studies confirmed the composition of the composites. The position of the G- and D-bands described the vibrational modes analogue to different bonds. The extent of defects and disorder was also calculated for the samples using I_D/I_G ratios. SEM images showed the layered structures with randomly aggregated PAni over the rGO, and hence confirmed the in situ polymerization of the composites. Cyclic voltammetry was carried out to validate the electrochemical performance of the composites. The samples underwent electrochemical diffusion with KOH as the electrolyte, giving the specific capacitance of the samples at different scan rates. The average specific capacitance calculated for the scan rates from 5 mV/s to 50 mV/s were 7.26 Fg^{-1} for PNGP40,12.84 Fg^{-1} for PNGP60, and 11.76 Fg^{-1} for PNGP80. The maximum specific capacitance of the PNGP60 among the three samples provided an idea of the optimum ratio of rGO and PAni in the composites.

Acknowledgments One of the authors Dr. Paramjit Singh is highly thankful to Science and Engineering Research Board (SERB), Department of Science and Technology, Government of India for providing financial assistance under Teachers Associateship for Research Excellence (TARE) Research Project (File No. TAR/2021/000128) to carry-out this research work. The characterization facilities provided by Malaviya National Institute of Technology (MNIT), Jaipur, India are gratefully acknowledged.

Funding The study was funded by Science and Engineering Research Board (SERB), Department of Science and Technology, Government of India under 'Teachers Associateship for Research Excellence' (TARE) Research Project (File No. TAR/2021/000128).

Conflict of interest The authors declare that they have no conflict of interest.

References

1. P. Forouzandeh, V. Kumaravel, and S.C. Pillai, Electrode materials for supercapacitors: a review of recent advances. *Catalysts* 10, 969 (2020). https://doi.org/10.3390/catal10090969.
2. J. Zhang and X.S. Zhao, Conducting polymers directly coated on reduced graphene oxide sheets as high-performance supercapacitor electrodes. *J. Phys. Chem. C* 116, 5420 (2012). https://doi.org/10.1021/jp211474e.
3. T. Kobayashi, H. Yoneyama, and H. Tamura, Oxidative degradation pathway of polyaniline film electrodes. *J. Electroanal. Chem. Interfacial Electrochem.* 177, 293 (1984). https://doi.org/10.1016/0022-0728(84)80230-2.
4. K. Wang, H. Wu, Y. Meng, and Z. Wei, Conducting polymer nanowire arrays for high performance supercapacitors. *Small* 10(1), 14 (2013). https://doi.org/10.1002/smll.201301991.
5. S. Yazar, M.B. Arvas, and Y. Sahin, S, N and Cl Separately doped graphene oxide/polyaniline composites for hybrid supercapacitor electrode. *J. Electrochem. Soc.* 169, 120536 (2022). https://doi.org/10.1149/1945-7111/acadb1.
6. Q. Cheng, J. Tang, J. Ma, H. Zhang, N. Shinya, and L.C. Qin, Polyaniline-coated electro-etched carbon fiber cloth electrodes for supercapacitors. *J. Phys. Chem. C* 115, 23584 (2011). https://doi.org/10.1021/jp203852p.
7. K. Chen, L. Chen, Y. Chen, H. Bai, and L. Li, Three-dimensional porous graphene-based composite materials: electrochemical synthesis and application. *J. Mater. Chem.* 22, 20968 (2012). https://doi.org/10.1039/c2jm34816k.
8. Z.D. Huang, R. Liang, B. Zhang, Y.B. He, and J.K. Kim, Evolution of flexible 3D graphene oxide/carbon nanotube/polyaniline composite papers and their supercapacitive performance. *Compos. Sci. Technol.* 88, 126 (2013). https://doi.org/10.1016/j.compscitech.2013.08.038.
9. A. Singh, J. Dhau, R. Kumar, R. Badru, P. Singh, Y.K. Mishra, and A. Kaushik, Tailored carbon materials (TCM) for enhancing photocatalytic degradation of polyaromatic hydrocarbons. *Prog. Mater. Sci.* 144, 101289 (2024). https://doi.org/10.1016/j.pmatsci.2024.101289.
10. M.M. Rahman, M.R. Shawon, M.H. Rahman, I. Alam, M.O. Faruk, M. Mizanur, R. Khan, and O. Okoli, Synthesis of polyaniline-graphene oxide based ternary nanocomposite for supercapacitor application. *J. Energy Storage* 67(1), 107615 (2023). https://doi.org/10.1016/j.est.2023.107615.
11. Y. Guo, J. Chang, L. Hu, Y. Lu, S. Yao, X. Su, X. Zhang, H. Zhang, and J. Feng, Hollow bowl NiS_2@polyaniline conductive linker/graphene conductive network: a triple composite for high-performance supercapacitor applications. *ChemSusChem* 17(3), e202301148 (2023). https://doi.org/10.1002/cssc.202301148.

12. J. Upadhyay, R. Borah, T.M. Das, and J.M. Das, Flexible solid-state supercapacitor based on ternary nanocomposites of reduced graphene oxide and ruthenium oxide nanoparticles bridged by polyaniline nanofibers. *J Energy Storage* 72(Part D6), 108600 (2023). https://doi.org/10.1016/j.est.2023.108600.
13. H. Xu, Z. Lei, M. Xu, J. Zhu, X. Song, and X. Jin, Free-standing reduced graphene oxide/carboxymethylcellulose-polyaniline (RGO/CMC-PAni) hybrid film electrode for high-performance asymmetric supercapacitor device. *Int. J. Biol. Macromol.* 236, 123934 (2023). https://doi.org/10.1016/j.ijbiomac.2023.123934.
14. M. Devi and A. Kumar, *In-situ* reduced graphene oxide nanosheets–polypyrrole nanotubes nanocomposites for supercapacitor applications. *Synth. Met.* 222, 15493 (2016). https://doi.org/10.1016/j.synthmet.2016.11.004.
15. Z. Liu, Z. Zhao, A. Xu, W. Li, and Y. Qin, Facile preparation of graphene/polyaniline composite hydrogel film by electrodeposition for binder-free all-solid-state supercapacitor. *J. Alloys Compd.* 875, 159931 (2021). https://doi.org/10.1016/j.jallcom.2021.159931.
16. N.I. Zaaba, K.L. Foo, U. Hashim, S.J. Tan, W.W. Liu, and C.H. Voon, Synthesis of graphene oxide using modified hummers method: solvent influence. *Procedia Eng.* 184, 469 (2017). https://doi.org/10.1016/j.proeng.2017.04.118.
17. W. Tang, L. Peng, C. Yuan, J. Wang, S. Mo, C. Zhao, Y. Yu, Y. Min, and A.J. Epstein, Facile synthesis of 3D reduced graphene oxide and its polyaniline composite for super capacitor application. *Synth. Met.* 202, 140 (2015). https://doi.org/10.1016/j.synthmet.2015.01.031.
18. F. Usman, J.O. Dennis, K.C. Seong, A.Y. Ahmed, F. Meriaudeau, O.B. Ayodele, A.R. Tobi, A.A.S. Rabih, and A. Yar, Synthesis and characterisation of a ternary composite of polyaniline reduced graphene-oxide and chitosan with reduced optical band gap and stable aqueous dispersibility. *Results Phys.* 15, 102690 (2019). https://doi.org/10.1016/j.rinp.2019.102690.
19. H. Gul, A.A. Shah, U. Krewer, and S. Bilal, Study on direct synthesis of energy efficient multifunctional polyaniline-graphene oxide nanocomposite and its application in aqueous symmetric supercapacitor devices. *Nanomaterials* 10, 118 (2020). https://doi.org/10.3390/nano10010118.
20. T.N. Mutalib, S.J. Tan, K.L. Foo, Y.M. Liew, C.Y. Heah, and M.M. Abdullah, Properties of polyaniline/graphene oxide (PAni/GO) composites: effect of GO loading. *Polym. Bull.* 78, 4835 (2021). https://doi.org/10.1007/s00289-020-03334-w.
21. A. Solonaru and M. Grigoras, Water-soluble polyaniline/graphene composites as materials for energy storage applications. *Express Polym. Lett.* 11, 127 (2017). https://doi.org/10.3144/expresspolymlett.2017.14.
22. S. Sultana, N. Ahmad, S.M. Faisal, M. Owais, and S. Sabir, Synthesis, characterisation and potential applications of polyaniline/chitosan-Ag-nano-biocomposite. *IET Nanobiotechnol.* 11, 835 (2017). https://doi.org/10.1049/iet-nbt.2016.0215.
23. J. Luo, S. Jiang, Y. Wu, M. Chen, and X. Liu, Synthesis of stable aqueous dispersion of graphene/polyaniline composite mediated by polystyrene sulfonic acid. *J. Polym. Sci. A Polym. Chem.* 50, 4888 (2012). https://doi.org/10.1002/pola.26316.
24. R.G. Bavane, M.D. Shirsat, and A.M. Mahajan, Ammonia gas sensing characteristics of chemically synthesized polyaniline matrix. *Sens. Transducers* 113, 63 (2010).
25. A.G. Tabrizi, N. Arsalani, H. Namazi, and I. Ahadzadeh, Vanadium oxide assisted synthesis of polyaniline nanoarrays on graphene oxide sheets and its application in supercapacitors. *J. Electroanal. Chem.* 798, 34 (2017). https://doi.org/10.1016/j.jelechem.2017.04.059.
26. R. Mahendran, D. Sridharan, K. Santhakumar, and G. Gnanasekaran, Green route fabrication of graphene oxide reinforced polymer composites with enhanced mechanical properties. *J. Nanosci.* 2016, 6410295 (2016). https://doi.org/10.1155/2016/6410295.
27. J. Song, X. Wang, and C.T. Chang, Preparation and characterization of graphene oxide. *J. Nanomater.* 2014, 276143 (2014). https://doi.org/10.1155/2014/276143.
28. N. Macherla, K. Singh, M.S. Santosh, K. Kumari, and R.G. Reddy Lekkala, Heat assisted facile synthesis of nanostructured polyaniline/reduced crumbled graphene oxide as a high-performance flexible electrode material for supercapacitors. *Colloids Surf. A Physicochem. Eng. Asp.* 612, 125982 (2020). https://doi.org/10.1016/j.colsurfa.2020.125982.
29. N.M. Soudagar, V.K. Pandit, V.M. Nikale, S.G. Thube, and S.S. Joshi, Influence of surfactant on the supercapacitive behaviour of polyaniline-carbon nanotube composite thin films. *ES Gener.* 2, 1018 (2023). https://doi.org/10.30919/esg1018.
30. P. Humpolíček, K.A. Radaszkiewicz, V. Kašpárková, J. Stejskal, M. Trchová, Z. Kuceková, H. Vičarová, J. Pacherník, M. Lehocký, and A. Minařík, Stem cell differentiation on conducting polyaniline. *RSC Adv.* 5, 68796 (2015). https://doi.org/10.1039/c5ra12218j.
31. M. Delvaux, J. Duchet, P.Y. Stavaux, M.R. Legras, and S.D. Champagne, Chemical and electrochemical synthesis of polyaniline micro-and nanotubules. *Synth. Met.* 113(3), 275 (2000). https://doi.org/10.1016/S0379-6779(00)00226-5.
32. M. Mitra, C. Kulsi, K. Chatterjee, K. Kargupta, S. Ganguly, D. Banerjee, and S. Goswami, Reduced graphene oxide-polyaniline composites—synthesis, characterization and optimization for thermoelectric applications. *RSC Adv.* 5, 31039 (2015). https://doi.org/10.1039/C5RA01794G.
33. W.I. Singh, S. Sinha, N. Aruna Devi, S. Nongthombam, S. Laha, and B.P. Swain, Investigation of chemical bonding and electronic network of rGO/PAni/PVA electrospunnanofiber. *Polym. Bull.* 78, 6613 (2021). https://doi.org/10.1007/s00289-020-03442-7.
34. R. Bhujel and B.P. Swain, Investigation of cyclic voltammetry and impedance spectroscopy of thermally exfoliated biomass synthesized nickel decorated graphene. *J. Phys. Chem. Solid* 130, 242 (2019). https://doi.org/10.1016/j.jpcs.2019.02.023.
35. Y. Zhang, J. Liu, Y. Zhang, J. Liu, and Y. Duan, Facile synthesis of hierarchical nanocomposites of aligned polyaniline nanorods on reduced graphene oxide nanosheets for microwave absorbing materials. *RSC Adv.* 7, 54031 (2017). https://doi.org/10.1039/c7ra08794b.
36. M.F. Mousavi, M. Hashemi, M.S. Rahmanifar, and A. Noori, Synergistic effect between redox additive electrolyte and PAni-rGO nanocomposite electrode for high energy and high power supercapacitor. *Electrochim. Acta* 228, 290 (2017). https://doi.org/10.1016/j.electacta.2017.01.027.
37. S.A. Chen and H.T. Lee, Polyaniline Plasticized with 1-Methyl-2-pyrrolidone: structure and doping behavior. *Macromolecules* 26, 3254 (1993). https://doi.org/10.1021/ma00065a002.
38. P. Liu and Y. Huang, Decoration of reduced graphene oxide with polyaniline film and their enhanced microwave absorption properties. *J. Polym. Res.* 21, 430 (2014). https://doi.org/10.1007/s10965-014-0430-7.
39. C. Dong, X. Zhang, Y. Yu, L. Huang, J. Li, Y. Wu, and Z. Liu, An ionic liquid-modified RGO/polyaniline composite for high performance flexible all-solid-state supercapacitors. *Chem. Commun.* 56(81), 1 (2020).
40. B. Rajagopalan and J.S. Chung, Reduced chemically modified graphene oxide for supercapacitor electrode. *Nanoscale Res. Lett.* 9, 535 (2014). https://doi.org/10.1186/1556-276X-9-535.
41. Y. Li and Y. Zheng, Preparation and electrochemical properties of polyaniline/reduced graphene oxide composites. *J. Appl. Polym. Sci.* 135, 46103 (2018). https://doi.org/10.1002/App.46103.
42. J. Xu, D. Wang, Y. Yuan, W. Wei, L. Duan, L. Wang, H. Bao, and W. Xu, Polypyrrole/reduced graphene oxide coated fabric

electrodes for supercapacitor application. *Org. Electron.* 24, 153 (2015). https://doi.org/10.1016/j.orgel.2015.05.037.
43. H. Liu, W. Zhang, H. Song, X. Chen, J. Zhou, and Z. Ma, Tremella-like graphene/polyaniline spherical electrode material for supercapacitors. *Electrochim. Acta* 146, 511 (2014). https://doi.org/10.1016/j.electacta.2014.09.083.